



# Importance of hydraulic strategy trade-offs in structuring response of canopy trees to extreme drought in central Amazon

Maquelle Neves Garcia<sup>1</sup> · Marciel José Ferreira<sup>2</sup> · Valeriy Ivanov<sup>3</sup> · Victor Alexandre Hardt Ferreira dos Santos<sup>1</sup> · João Vitor Ceron<sup>1</sup> · Alacimar Viana Guedes<sup>1</sup> · Scott Reid Saleska<sup>4</sup> · Rafael Silva Oliveira<sup>5</sup>

Received: 30 October 2020 / Accepted: 21 April 2021

© The Author(s), under exclusive licence to Springer-Verlag GmbH Germany, part of Springer Nature 2021

## Abstract

Plant ecophysiological trade-offs between different strategies for tolerating stresses are widely theorized to shape forest functional diversity and vulnerability to climate change. However, trade-offs between hydraulic and stomatal regulation during natural droughts remain under-studied, especially in tropical forests. We investigated eleven mature forest canopy trees in central Amazonia during the strong 2015 *El Niño*. We found greater xylem embolism resistance ( $P_{50} = -3.3 \pm 0.8$  MPa) and hydraulic safety margin ( $HSM = 2.12 \pm 0.57$  MPa) than previously observed in more precipitation-seasonal rainforests of eastern Amazonia and central America. We also discovered that taller trees exhibited lower embolism resistance and greater stomatal sensitivity, a height-structured trade-off between hydraulic resistance and active stomatal regulation. Such active regulation of tree water status, triggered by the onset of stem embolism, acted as a feedback to avoid further increases in embolism, and also explained declines in photosynthesis and transpiration. These results suggest that canopy trees exhibit a conservative hydraulic strategy to endure drought, with trade-offs between investment in xylem to reduce vulnerability to hydraulic failure, and active stomatal regulation to protect against low water potentials. These findings improve our understanding of strategies in tropical forest canopies and contribute to more accurate prediction of drought responses.

**Keywords** Hydraulic vulnerability · *El Niño* · Stomatal conductance · Safety margin · Climate change

## Introduction

Communicated by Kate McCulloh.

We found tradeoffs between stomatal regulation and hydraulic safety in individuals Amazon trees facing extreme drought. This is novel for tropical forests, and provides new insight into potential climate change responses in a seasonally wet tropical ecosystem that is particularly at risk during El Niño climate events.

✉ Maquelle Neves Garcia  
maquelleneves@gmail.com

<sup>1</sup> Coordination of Environmental Dynamics,  
National Institute of Amazon Researches, Manaus,  
Amazonas (AZ) 69067-375, Brazil

<sup>2</sup> Department of Forest Sciences, Federal University  
of Amazonas, Manaus, Amazonas (AZ) 69067-005, Brazil

<sup>3</sup> Department of Civil and Environmental Engineering,  
University of Michigan, Ann Arbor, MI 48109, USA

<sup>4</sup> Department of Ecology and Evolutionary Biology, University  
of Arizona, Tucson, AZ 85721, USA

<sup>5</sup> Plant Biology Department, University of Campinas,  
Campinas, São Paulo 13083-970, Brazil

Tropical forests cover 10% of the global surface, stock 25% of the world's carbon, and are responsible for a third of the global net primary productivity (Malhi et al. 1998; Crowther et al. 2015). Through changes in temperatures and precipitation, climate change might potentially lead to a decrease in productivity of forests and increase tree mortality (Allen et al. 2015), as has already been reported for different biomes (Phillips et al. 2009, 2010; Anderegg et al. 2016; McDowell et al. 2018). In tropical forests, tree mortality is linked to reduced forest productivity and has been related mainly to the occurrence of extreme drought events (Doughty et al. 2015; Brienen et al. 2015; Aleixo et al. 2019). Such episodes have the potential to severely alter the composition of plant communities and thus modify forest functional characteristics at the ecosystem level (McDowell et al. 2018). However, unlike in other global biomes that have experienced massive die-off events (McDowell et al. 2015; Fettig et al. 2019) or strong mortality responses to drought (Venturas et al 2016), mortality events in tropical Amazon rainforests observed

so far have been more subtle and nuanced, highlighting the need to better understand mechanisms of drought tolerance in Amazon forests.

In 2015, a severe drought occurred across large areas of the Amazon. It was associated with the *El Niño*/Southern Oscillation (ENSO), breaking the records of previous extreme drought events in 2005, 2010, and 1997–1998 *El Niño*, the strongest in the modern record for central Amazonia (Jiménez-Muñoz et al. 2016). This 2015 drought provided a unique opportunity—a natural drought experiment—to investigate hydraulic traits associated with mechanisms of drought tolerance. Specifically, both structural and physiological traits involved in tree drought tolerance can be of interest: (i) xylem embolism resistance traits, which quantify the thresholds of tree hydraulic integrity under water deficit (Mitchell et al. 2013), and (ii) stomatal conductance regulation, which controls water and carbon gas exchange at the leaf surface as well as the level of xylem tension (Sperry 2000). Stomatal closure in response to water deficit represents a cost in terms of carbon assimilation, plant growth, and temperature regulation (Lloyd and Farquhar 2008); furthermore, it has been already observed to be the primary cause of reduced photosynthesis rates in central Amazonian trees during 2015 *El Niño* (Santos et al. 2018).

Theoretical work seeks to improve predictions of woody plant response to drought by appropriately integrating xylem embolism resistance with stomatal conductance regulation into models (Sperry and Love 2015; Anderegg et al. 2018; Wu et al. 2019). Observations and experiments are being used to test such theories (see citations in Wang et al., 2020), but evidence from the tropics is more limited. Previous tropical forest field experiments in which trees were subjected to a partial exclusion of rainfall showed that taxa with traits associated with lower xylem embolism resistance had higher drought-induced mortality rates (Rowland et al. 2015a), supporting the hypothesis that xylem hydraulic traits might explain cross-species patterns of drought-induced mortality (Anderegg et al. 2016). However, neither the Rowland et al. (2015a) study of an experimental drought, nor other studies of hydraulic responses of tropical trees to natural drought (Fontes et al. 2018; Barros et al. 2019) were able to explicitly observe whether stomatal response co-varies with embolism resistance at the individual level, a key prediction of the theory that remains untested in tropical forests. A goal of this work is, thus, to investigate the extent to which xylem susceptibility to embolism can be counterbalanced by active stomatal regulation under natural drought conditions—a key knowledge gap since such a trade-off determines the limits of physiological functioning under drought stress (Fauset et al. 2019; Wang et al. 2020).

Closely related is the question of whether the emergent hydraulic safety margins (HSM) measured in this forest during an extreme drought are consistent with the growing

database of HSMs around the world. HSM, a measure used to assess the capacity of a species' hydraulic system to resist embolism that has been shown an effective predictor of tree mortality during drought (Anderegg et al. 2016; Powers et al. 2020), is estimated as the difference between the water potential at which the plant loses 50% of hydraulic conductivity ( $P_{50}$ ) and the minimum water potential ( $P_{\min}$ ) observed in the field. A common interpretation is that the likelihood for a hydraulic system to suffer embolism is lower for larger magnitudes of HSM. A global-scale survey found small HSMs for angiosperms around the global biomes, despite the wide variation in absolute measures of embolism vulnerability such as  $P_{50}$  (Choat et al. 2012). Global convergence to a common HSM suggests that forest biomes would be equally vulnerable to hydraulic failure across a range of precipitation environments. The extreme drought conditions of the 2015 *El Niño* event provide an ideal opportunity to observe  $P_{\min}$  and the associated HSM outside of the range of 'normal' tree function and to test the robustness of tree hydraulic system to embolism. Literature reporting hydraulic safety margins and  $P_{\min}$  data for drought (Brum et al. 2019) and non-drought conditions (Choat et al. 2012) provides the needed background to compare HSM from different forests.

Here, we ask two main questions: (1) Is the hydraulic safety margin observed for central Amazon canopy trees during a severe natural drought event consistent with what had been previously observed for tropical trees? (2) What are the trade-offs between stress-tolerance mechanisms in tropical forest trees subjected to a strong natural drought? We hypothesize that canopy trees in central Amazon operate under lower hydraulic safety margins because stomata operate at the edge of the supply capacity of the plant's hydraulic system to balance carbon uptake and leaf temperature regulation during drought.

## Materials and methods

### Study site, species, and experimental design

We conducted our study in a central Amazon forest at the Large-Scale Biosphere–Atmosphere (LBA) Experiment in Amazonia K-34 tower site (2.59° S, 60.21° W). The average annual precipitation is 2600 mm (1998–2014), with dry season defined as the months with  $< 100$  mm month $^{-1}$ , typically occurring between July and October (Sombroek 2001). Air temperature ranges within 24–27 °C and relative humidity is 75–92% (Araújo et al. 2002). During the dry season of years without drought anomalies, soil water content (the top 30 cm layer) usually drops ~ 12% relative to the absolute magnitude of the wet season (Cuartas et al. 2012).

We measured traits for eleven individual canopy dominant trees of nine species (Table S1). The intent was to

sample a representative distribution of traits in the community, and infer drought responses in terms of trade-offs among the traits. Since the logistics of making measurements high in the canopy of diverse tropical forests severely limit ability to sample the taxonomic diversity of species, and to carry out effective replication (since conspecific are often spaced tens to hundreds of meters apart), differences in species responses are not distinguished. However, a comparison to larger, community-scale datasets from the study region (across 261 individuals in central Amazon) suggests that forest canopy functional variability was well represented in terms of at least one of the key ecophysiological traits, specifically, leaf mass per area (LMA, see supplemental Fig. S1).

We made measurements in four campaigns, capturing seasonal variation of tree function across May, July, September, and October 2015. Sampled trees were accessed from a 30-m long walkway installed 25 m above the ground. Three species, *Eschweilera truncata*, *Licania micrantha*, and *Scleronema micranthum*, are among hyperdominant species in the Amazon, contributing a large biomass fraction in the region (ter Steege et al. 2013; Fauset et al. 2015). The trees were located in the proximity to the energy and carbon eddy-flux tower (K-34) in the *terra firme* (i.e., topographic high) region of the watershed that has seasonally deep groundwater (~37 m) (Cuartas et al. 2012).

### Environmental conditions during 2015 El Niño event

Monthly precipitation series were analyzed for the period of 1998–2015, while relative humidity, air temperature, and soil moisture for the year of 2015. The data were obtained from the LBA/K-34 site database. Soil moisture was observed at six depths (10, 20, 30, 40, 60, and 100 cm) during May, July, September, and October of 2015 (PR1, Delta-T Devices, UK). Precipitation data were used to calculate the maximum climatological water deficit (CWD). Specifically, CWD is a cumulative sum of the difference between monthly rainfall and evapotranspiration with the negative difference implying water deficit (Aragão et al. 2007; Malhi et al. 2009).

To demonstrate the *El Niño* impact on central Amazon climate, the maximum air temperature (obtained from a station managed by the Brazilian National Institute of Meteorology, INMET Manaus station, 3.13° S; 59.95° W) and precipitation anomalies were calculated (Saleska et al. 2007), and as a function of the multivariate *El Niño* Index for the period of 1998–2015 (MEI, National Ocean and Atmospheric Administration web-site, [https://psl.noaa.gov/site\\_index.html](https://psl.noaa.gov/site_index.html)).

### Diurnal and seasonal leaf water potential measurements

Leaf water potential was measured with a pressure chamber model 3005–1422 (Soil Moisture Equipment Corp, USA), following the protocol of Scholander et al. 1964; Turner 1981. Sampled trees were accessed from the walkway and the measurements were performed directly in the canopy. Only mature, healthy, and fully expanded leaves with no signs of aging or senescence and exposed to sunlight were selected for the measurements. We evaluated the diurnal variation of leaf water potential by making measurements on three leaves per individual, six times during the day (at hours 6:00, 8:00, 10:00 12:00, 14:00, and 16:00), of which we consider the measurements at 6:00 as representative of predawn water potential ( $P_{pd}$ ) and at 12:00 as midday water potential ( $P_{md}$ ). The sampled leaves were collected and immediately placed into a pressure chamber, which was moistened with a piece of tower paper to prevent water loss during the measurements (Turner 1981). The four measurement campaigns captured seasonal variation across each of the months of May, July, September, and October 2015 (Fig. S2).

### Xylem vulnerability

For each of the eleven trees, three branches were collected between March and April 2016. At predawn, long branches (see details in Fig. S3) were collected using an 8-m long pole-pruner standing on a canopy walkway. We sampled branches exposed to sunlight, reaching 95%–100% of the total height for all of the eleven trees. The collected branches were kept in black humidified plastic bags prior to the measurement session to ensure the maintenance of water potential. The samples were brought back to the lab within 1 h of branch collection. Tree embolism resistance was measured with the pneumatic method (Pereira et al. 2016; Zhang et al. 2018). The vulnerability curve was obtained by plotting the percent loss conductivity (PLC) in response to declining xylem water potential ( $\Psi_x$ ). We subsequently bench dried branches to a range of  $\Psi_x$  values which were measured using a Scholander pressure chamber (PMS, Pressure Chamber Instrument, Oregon, USA). Measurements were made on 2–3 branches per individual tree. Before each measurement, we bagged branches for 40 min to equilibrate the xylem water potential. To calculate  $P_{50}$  and  $P_{12}$  (the “air-entry” point water potential, commonly used as an estimate of the xylem tension at which pit membranes within the conducting xylem are overcome with air seeds, indicating the start of embolism), we fitted a nonlinear two-parameter Weibull equation (Eq. 1):

$$\text{PLC} = 1 - e^{-(\Psi_x/b)^k}, \quad (1)$$

where  $\Psi_x$  is the xylem water potential,  $b$  is the scale parameter and  $K$  are the shape parameters estimated. The coefficients were estimated using nonlinear least-squares fitting with the optimx function of the optimx package in R (R Development Core Team 2011).

## Hydraulic safety margin

Hydraulic safety margin (HSM) was computed as the difference between the midday leaf water potential ( $P_{\text{md}}$ ) of the plant reached during the drought and  $P_{50}$ . We compared the observed central Amazon tree HSMs during extreme drought with HSMs observed in eastern Amazon trees during the extreme *El Niño* drought of 2015 (Brum et al. 2019), and central American trees with seasonal droughts (Choat et al. 2012). See details in Supplementary Information (Table S2). Note that the Choat et al. 2012 data set used different methods for estimating the  $P_{50}$  component of the HSM than those used in this study (the pneumatic method based on Pereira et al. 2016). Much evidence supports the inter comparability of these methods (Zhang et al. 2018), while some (Pratt et al. 2020) report that the pneumatic method may produce a relatively lower magnitude of  $P_{50}$  and HSM in some cases.

## Leaf gas exchange

Stomatal conductance ( $g_s$ ), leaf transpiration ( $E$ ), and photosynthetic rate ( $A_{\text{sat}}$ ) were measured in situ in leaves attached to branches using a portable infrared gas analyzer (LI-COR 6400XT, Nebraska, USA). Only mature, healthy, and fully expanded leaves with no signs of aging or senescence and exposed to sunlight were selected for the measurements. Sampling heights ranged from 77 to 100% of the maximum tree height in the sample (32.5 m), with leaves of seven trees sampled at their full heights. Four leaves per tree were measured each day and each individual leaf was measured every 2 hours during the diurnal course (at 8:00, 10:00, 12:00, and 14:00). In total, 176 leaves were measured (4 leaves/tree/day  $\times$  11 trees  $\times$  4 days, i.e., 2 days during pre-drought and 2 days during drought). Each leaf was allowed to acclimate for  $10 \pm 5$  min before each measurement. To exclude the impact of variability in leaf ambient environment, and focus on how seasonal evolution of leaf gas exchange depended on the xylem and soil water status, each measurement was carried out in controlled conditions. Specifically, the gas analyzer was set up for a saturating photon flux density (PPFD) of  $2000 \mu\text{mol m}^{-2} \text{ s}^{-1}$ , air flow of  $400 \mu\text{mol s}^{-1}$ ,  $\text{CO}_2$  concentration of  $400 \mu\text{mol mol}^{-1}$ , leaf temperature of  $31^\circ\text{C}$ , and  $\text{H}_2\text{O}$  vapor concentration of  $21 \text{ mmol mol}^{-1}$  (as in Santos et al. 2018). We note that our approach of setting the measurement chamber environment to common reference conditions is a standard practice across many studies (Resco

et al. 2009; Stpaul et al. 2012; Chmura et al. 2015; Li et al. 2015; Hernandez-Santana et al. 2016) especially for those that focus, as we do here, on the regulatory effects of soil and xylem water conditions. This design, however, likely underestimates the full drought effect on leaf gas exchange in the forest, as the leaf gas exchange measurements take place in a moderate environment in between the in situ extremes experienced in wet or dry seasons. To the extent that we nonetheless discern effects of drought, we consider these findings to be conservative.

## Relative changes in gas exchanges during the El Niño

To understand the dynamics of stomatal control, we quantified the sensitivity of *El Niño*-induced changes in  $g_s$  by computing its difference between dry and wet periods ( $\delta g_s$ ). Specifically, the ‘wet’ reference condition was taken as the maximum value of  $g_s$  recorded in May and July of 2015 (measurements at 8:00 or 10:00) and the ‘dry’ *El Niño* condition corresponded to October 2015 (also at 8:00 or 10:00). A negative  $\delta g_s$  value means a reduction in stomatal conductance. Also, we calculated the intrinsic water-use efficiency ( $i\text{WUE} = A_{\text{sat}}/g_s$ ) in May, July, September, and October.

## Wood density, DBH, and height

We measured wood density with the water-displacement method using three branch segments (2–4 cm in diameter) of each tree. After removal of the outer bark, the volume was estimated from the saturated samples that remained immersed in distilled water for 12 h to ensure complete saturation. We calculated density using the dry mass ratio (at  $105^\circ\text{C}$ ) of branch segments by the volume. For diameter at breast height (DBH) measurements, the tree circumference was measured at 1.30 m above ground level using a 5 m diameter tape (Forestry Supplies, Mississippi, USA). The tree height was obtained with a measure tape using climbing techniques.

## Statistical analysis

To test the differences between hydraulic safety margin estimated for trees in central Amazon and other sites, we used analysis of variance (ANOVA) for averages with different repetitions (see details in Table S2) and compared sites using planned contrasts (Field 2018). We tested the main effects of seasonality on stomatal ( $g_s$ ), leaf transpiration ( $E$ ), photosynthetic rate ( $A_{\text{sat}}$ ), and intrinsic water-use efficiency ( $i\text{WUE}$ ) with generalized linear mixed models (GLMM): months as the fixed effect, and trees as the random effect. We compared wet (May and July) vs. dry (September and October) seasons

with planned contrasts. To test the sphericity assumptions, we used the Mauchly test (Field 2018).

To investigate possible trade-offs between stomatal control and embolism resistance, we used generalized linear models (GLM). To test the importance of stomatal control for keeping the minimum water potential at safe levels during the drought peak, we tested a relationship between the minimum water potential ( $P_{\min\text{loct}}$ ) vs.  $g_s$  in October. To investigate a possible connection between stomatal control during the dry season and the plant hydraulic system, we tested the effect of the “air-entry” water potential  $P_{12}$  on  $\delta g_s$ .

We used a nonlinear relationship between stomatal control ( $\delta g_s$  as  $y$ ) and tree height (as  $x$ ):  $y = -a + b * \exp(-c(x - 19))$ . We used *t.test* and *nls* functions, and *lme4* package (Bates and Maechler 2007) in R for computing all of the statistical tests in the data analysis (R Development Core Team 2011).

## Results

### Environmental conditions during 2015 El Niño event

The 2015 *El Niño* was the most severe drought at the study site in recent years. Precipitation during the dry season decreased to 36 mm in August, 27 mm in September, and 59 mm in October, reaching the lowest CWD in the recorded history (Fig. S4a). The overall reduction of annual precipitation in 2015 was around 800 mm, nearly 30% lower as compared to the historical mean of 2600 mm over the 1998–2015 period, extending the dry season to 5 months (Fig. S4a). The warmest period occurred between September and October 2015, and the average air temperature (37 °C) was higher than what was observed during the previous two strongest droughts on record in this region: by 1.5 °C as compared to the drought conditions in October 1997, and by 3.0 °C in January 1983. The extreme conditions of 2015 reduced soil water availability by 23% in comparison to the preceding rainy months (Fig. S4b). The temperature increases and the reduction in air humidity led to a high atmospheric vapor pressure deficit (4.4 kPa) (Fig. S4c). Anomalies of precipitation (Fig. S4d) and temperature (Fig. S4e) at the study site were correlated with the 2015 *El Niño* event intensity represented by MEI (i.e., the Multivariate ENSO index).

### Seasonality of leaf water potential and hydraulic safety margin

For all trees, leaf water potential exhibited strong diel and seasonal changes in 2015. We found that daily minimum water potential ( $P_{\min}$ ) did not always happen at midday ( $P_{\text{md}}$ ), nor did annual minimum happen during seasonal drought peak ( $P_{\min\text{Oct}}$ ), as might have been expected (Fig. 1).

The average predawn leaf water potential ( $P_{\text{pd}}$ , a proxy for root zone soil water potential) was 57.5% lower during the dry season drought peak ( $-0.4 \pm 0.2$  MPa in October versus an average of  $-0.17 \pm 0.02$  MPa during the May–July wet season), consistent with precipitation (CWD)-defined drought (Fig. S4a). However, midday water potential  $P_{\text{md}}$  was 20% higher (more hydrated) during the dry season when compared to the wet season (Fig. 1, upper left panel). During the CWD-defined drought peak (October), minimum leaf water potential  $P_{\min\text{Oct}}$  (average of  $-1.15 \pm 0.43$  MPa across all trees) occurred around 10am, and was slightly lower than midday water potential  $P_{\text{mdOct}}$  (average of  $-0.98 \pm 0.45$  MPa; Fig. 1). Note that when considering all months, the overall  $P_{\min}$  and  $P_{\text{md}}$  averages across all trees were  $-1.7 \pm 0.5$  MPa and  $-1.22 \pm 0.35$ , respectively, both lower than in October, emphasizing that the lowest measured leaf water potentials occurred prior to the October peak of climatic drought.

The average of xylem embolism resistance ( $P_{50}$ ) was  $-3.3 \pm 0.8$  MPa, similar to the values reported for a site with a higher seasonality in the eastern Amazon (Fig. 2a). During the peak of drought (October),  $P_{\text{md}}$  observations of central Amazonian trees (from this study) were similar to magnitudes observed in trees in central America (Choat et al. 2012) under non-drought conditions (Fig. 2b). Considering the seasonal water potential behavior we calculated the average hydraulic safety margins (HSMs) in central Amazon trees, considering  $P_{\min}$  ( $1.5 \pm 0.61$  MPa),  $P_{\min\text{Oct}}$  ( $2.0 \pm 0.55$  MPa), and  $P_{\text{md}}$  in October ( $2.1 \pm 0.57$  MPa). Overall, HSM was greater than what had been observed for other tropical rainforests ( $0.5 \pm 0.77$  MPa) (Fig. 2c, d). As we noted in the methods, the HSM method used in some of the other tropical forests (as reported in Choat et al 2012) was different than that used here, but the different methods have been found to be consistent (as reported in Zhang et al 2018); others report that the methods are inconsistent, and that the method used here may underestimate the magnitude of the HSM (Pratt et al. 2020), in which case the difference reported in Fig. 2c would be even larger and our finding of a high HSM and conservative operating strategy would still have strong support.

### Coordination between hydraulic and stomata traits

We found four main relationships that represent coordination between hydraulic and stomatal traits. First, more negative minimum water potential during the year  $P_{\min}$  and during drought ( $P_{\min\text{Oct}}$ ) (Fig. 2e) was associated with higher xylem embolism resistance (more negative  $P_{50}$ ), as would be expected if trees that endure greater hydraulic risk (more negative  $P_{\min\text{Oct}}$ ) are structured to have greater hydraulic safety (more negative  $P_{50}$ ).

Second, seasonal increases in intrinsic water-use efficiency (iWUE) indicate that photosynthesis declined

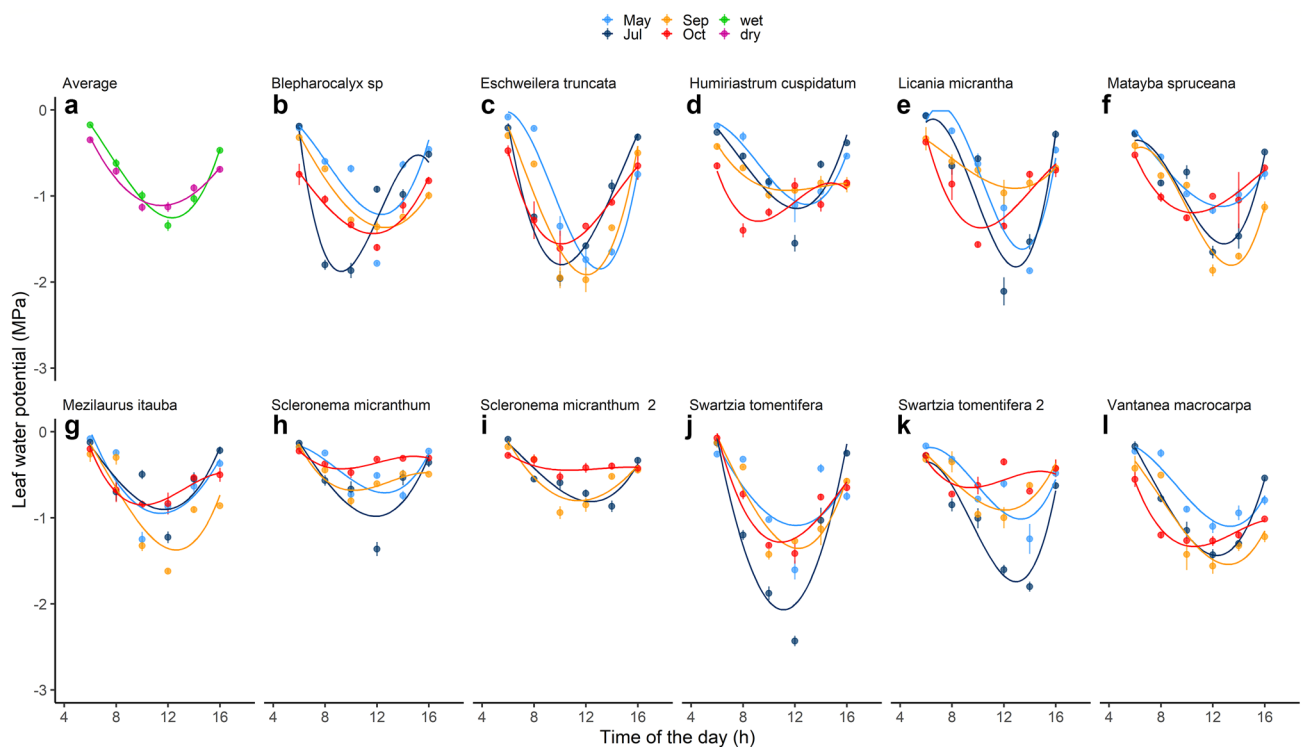


**Fig. 1** Composite diel patterns **a** for the wet (May, July;  $n=63$ ) and dry (September, October;  $n=66$ ) season months represent averages  $\pm$  SE. Diel average  $\pm$  standardized error (SE) of leaf water potential for each of the eleven studied trees during each of the four seasonal measurement campaigns (in May, July, September, and October of 2015;  $n=3$ ), capturing the evolution of the *El Niño* event **(b–l)**.

The predawn (6 am) average was low in the dry season ( $p=0.0029$ ), while the minimum water potential in the dry season was higher in comparison to the wet season ( $p=0.0024$ , paired  $t$  test on dry vs. wet season differences,  $n=11$  trees). Smoothed lines through observations allow visualization of distinct diel patterns for each tree and month (or season)

proportionally less than stomatal conductance for most trees (Fig. 2f). Likewise, the seasonal changes in assimilation ( $A_{\text{sat}}$ ) and transpiration ( $E$ ) can be observed directly: dry season  $E$  reduced by 48% and  $A_{\text{sat}}$  only by 40% (Fig. S5). At the same time, stomatal conductance was found to be inversely related to  $P_{\text{minOct}}$  (Fig. 3a). This suggests that drought conditions (as reflected in  $P_{\text{minOct}}$ ) are linked through hydraulic regulation (stomatal conductance) to the carbon assimilation and hydration level of these trees.

Third, we found key trade-offs among hydraulic traits across individuals that support a central tenet of hydraulic regulation theory that stomatal conductance regulation is closely linked to hydraulic safety in structuring strategies for drought response. In particular we observed a trade-off such that trees with more hydraulic vulnerability (with a higher water potential at which embolism starts, i.e., less negative “air-entry” point  $P_{12}$ ) were also those that more tightly regulated water loss through stoma (i.e., had greater decline in stomatal conductance,  $\delta g_s$ ) between wet and dry seasons (Fig. 3b).

Finally, higher embolism resistance (i.e., less negative  $P_{50}$ ) is found to be positively related to tree height and

diameter at breast height (DBH) (Fig. 4a, b). Concurrently, there is a negative relationship between the drought-induced stomatal conductance reduction and tree height (Fig. 4c), suggesting a height-structured trade-off between hydraulic safety and stomatal regulation.  $P_{50}$  was also found to be negatively related to wood density (Fig. 4d). Thus, smaller trees with more dense wood tended to be hydraulically safer and use less stomatal regulation.

## Discussion

Ecophysiological measurements carried out on trees subjected to one of the strongest droughts recorded in central Amazon resulted in two key findings that address the questions posed in the introduction: first, the unexpectedly high hydraulic safety margins in central Amazonian trees, and second, strong evidence for trade-offs between hydraulic safety and stomatal regulation, which has been widely hypothesized but not previously seen as tradeoffs in tropical forests across individuals. We discuss these two findings, as well as a third one that points to a likelihood of

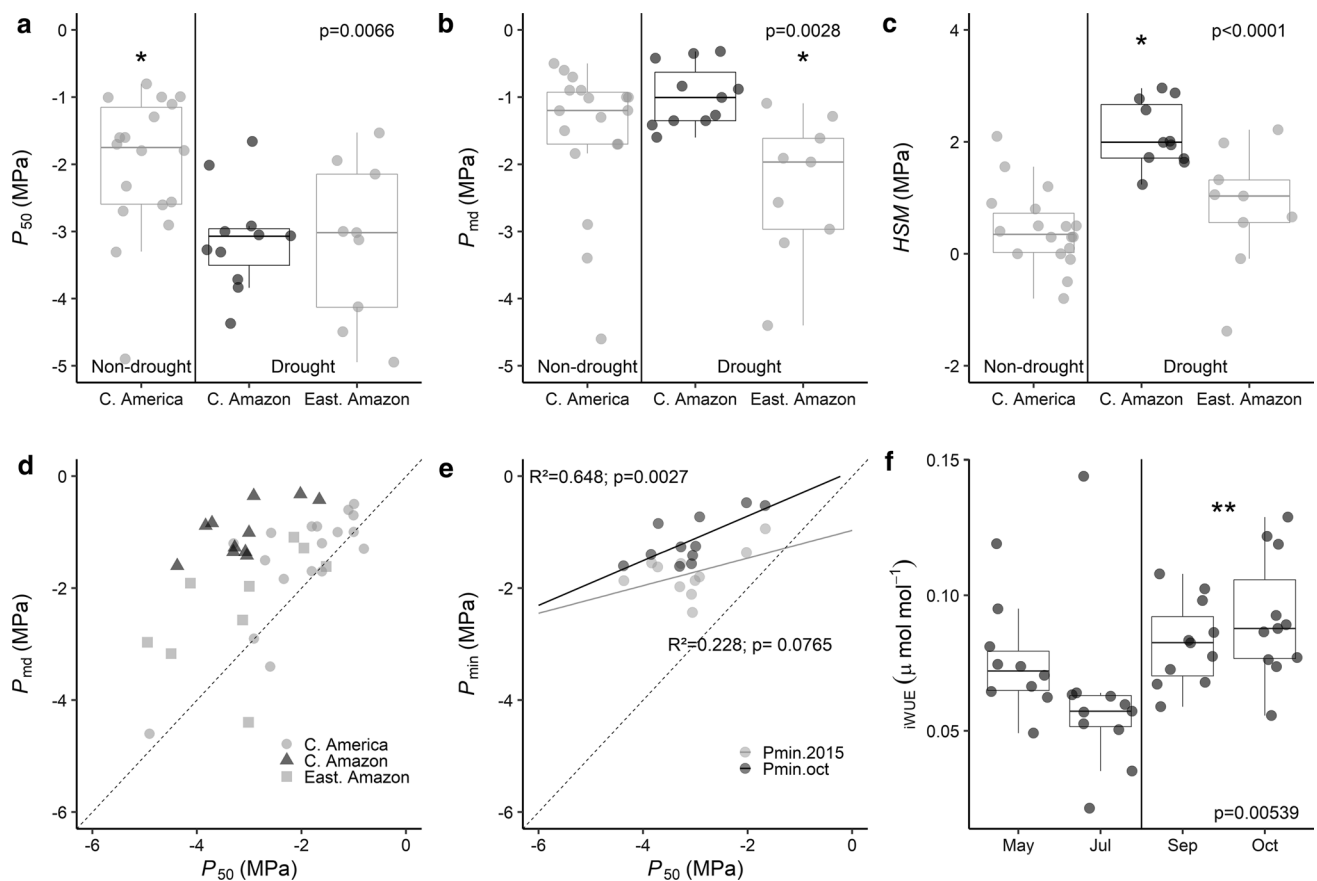


**Fig. 2** Hydraulic traits observed in this central Amazon (“C. Amazon”) study (in dark symbols) compared to other tropical studies in central America (“C. America”) and in the Eastern Amazon (“E. Amazon”) (a–d) and hydraulic trait dynamics among the 11 trees in this study (e, f): **a** Water potential at which plant loses 50% of hydraulic conductivity ( $P_{50}$ ) and **b** Midday leaf water potential  $P_{md}$  in trees from the central Amazon (this study, dark grey), as compared to data for central America (Choat et al. 2012), and Eastern Amazon (Brum et al. 2019). **c** Hydraulic safety margin (HSM) of trees from central Amazon (this study), central America (Choat et al. 2012), and Eastern Amazon (Brum et al. 2019). The species with replicate samples (two of the nine species) from this study were represented by their average values so the boxplot represents the distribution of species-specific values. **d** Leaf water potential (taken as  $P_{md}$ ) vs.

$P_{50}$ , showing greater HSM (greater vertical distance between sample points and 1:1 line) at this site (dark points) than in other studies (lighter points); **e** Minimum water potential in October 2015 ( $P_{min,Oct}$ ), and minimum water potential over the entire 2015 ( $P_{min}$ ) versus  $P_{50}$ , showing that drought-period hydraulic safety margin (HSM, the vertical distance between each point and the 1:1 dashed line) is greater than HSM estimated for the entire 2015. **f** Seasonal dynamics of intrinsic water-use efficiency (iWUE). The asterisk symbol (\*) denotes data significantly different from the planned orthogonal contrasts. Boxplots in panels a–c, f represent the data distributions as the median (central horizontal line), the interquartile range (top and bottom lines of each box), and the range of the data (whiskers) up to 95th percentile

a height-structured trade-off between resistance to xylem embolism and its active stomatal regulation.

### Do canopy trees in central Amazon have a narrow hydraulic safety margin?

Hydraulic safety margins (HSM) of central Amazon trees are larger than that of the trees located at an eastern Amazonia site with more pronounced precipitation seasonality (Brum et al. 2019). There are two factors determining HSM that define drought susceptibility of a given species: the intrinsic ability of xylem tissue to tolerate embolism ( $P_{50}$ ) and the lowest level of leaf hydration experienced by

the plant in the field ( $P_{md}$ ). *A priori*, we hypothesized that canopy trees in the central Amazon would operate with small HSMs, in accordance with the proposed global convergence in the vulnerability of forests to drought (Choat et al. 2012). Moreover, we also expected a decrease of  $P_{md}$  during the 2015 *El Niño* event which in turn would further decrease the safety margin. Contrary to the expectations, the studied canopy trees in central Amazon showed high HSMs, both in absolute magnitude (Ziegler et al. 2019) and in comparison to what previous studies have demonstrated (Fig. 2c, d). This was due to both the less negative  $P_{md}$  than expected—similar to observations in tropical rainforest in central America, (Fig. 2b)—and a relatively

**Fig. 3** Key hydraulic trait trade-offs: **a** between minimum water potential ( $P_{\min|Oct}$ ) and stomatal conductance in October; **b** between stomatal regulation (drought-induced change in stomatal conductance,  $\delta g_s$ ) and hydraulic safety (air-entry point water potential,  $P_{12}$ ). Lines are the predictions of GLMM fits between the two variables on the axes (see statistics method section)

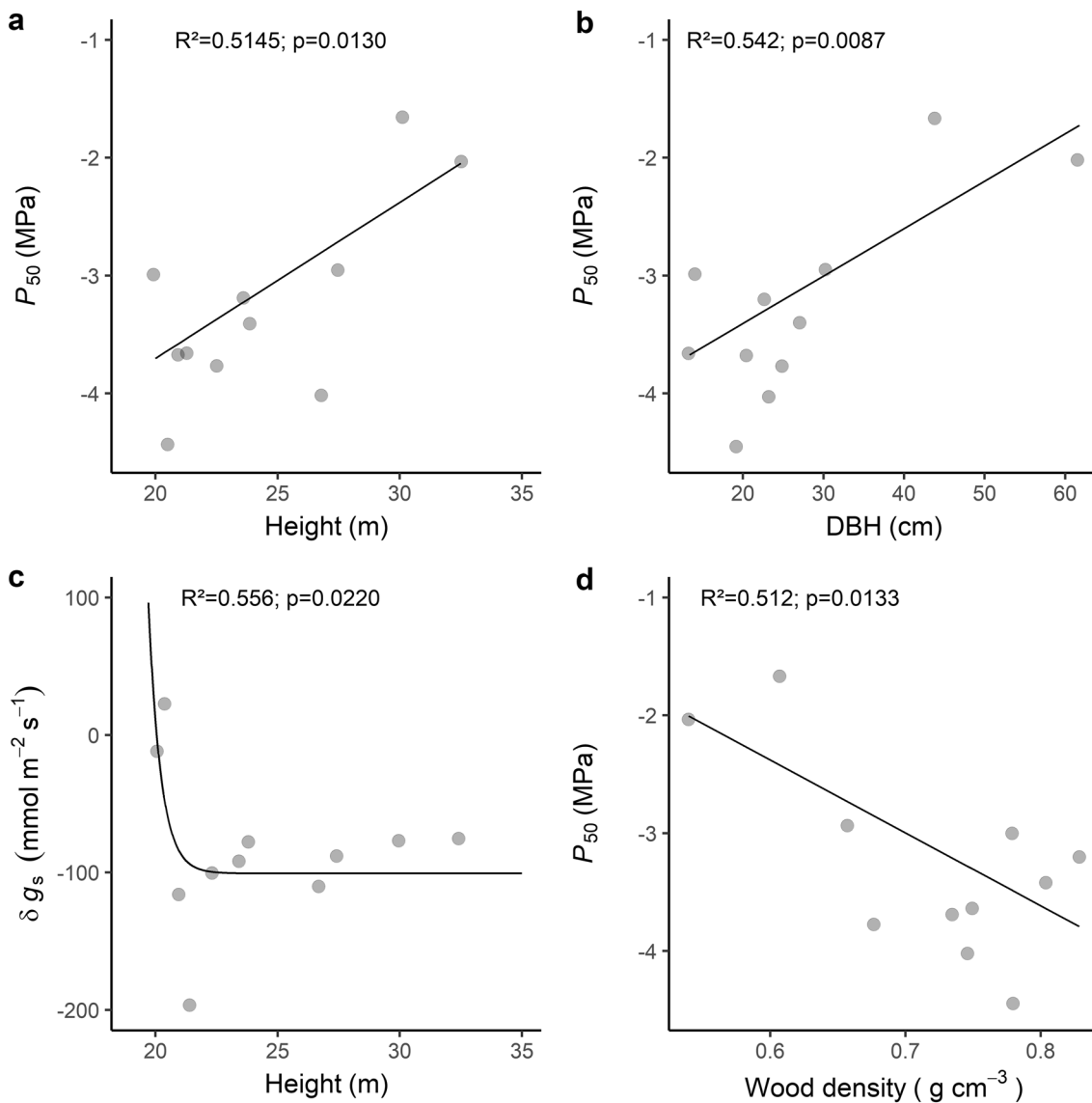
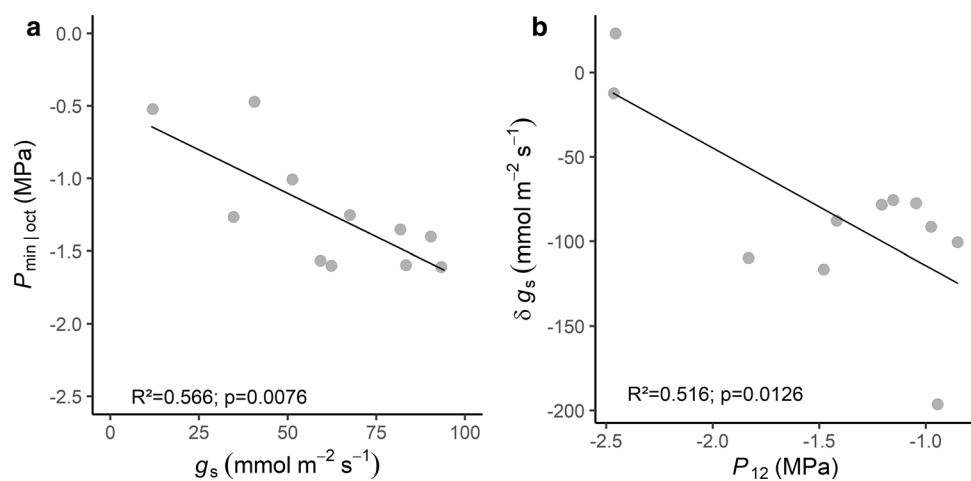


**Fig. 4** Key relations between hydraulic traits and tree size (a–c) and wood density (d):  $P_{50}$  (xylem water potential which plant loses 50% of hydraulic conductivity) versus: **a** tree crown height and **b** diameter at breast height (DBH). **c** Degree of stomatal regulation (drought-induced change in stomatal conductance,  $\delta g_s$ ) versus tree height, fitted with the nonlinear least-squares line  $y = -100.7 + 801 * \exp(-1.98(x - 19))$ . **d**  $P_{50}$  versus branch wood density

lation (drought-induced change in stomatal conductance,  $\delta g_s$ ) versus tree height, fitted with the nonlinear least-squares line  $y = -100.7 + 801 * \exp(-1.98(x - 19))$ . **d**  $P_{50}$  versus branch wood density

high resistance of xylem tissues to embolism (i.e., more negative  $P_{50}$ , Fig. 2a), with magnitudes similar to those observed at a more pronounced seasonal water deficit site located in the eastern Amazonia (Brum et al. 2019). One may note that if the minimum leaf water potential achieved during drought peak ( $P_{\min|Oct}$ ) is used to compute HSM, safety margins would be larger than those estimated with the overall  $P_{\min}$  (i.e., comparing the vertical distances from the two sets of symbols to the dashed line in Fig. 2e). This suggests that plants can increase HSM during a drought (if one considers  $P_{\min}$ ,  $P_{\min|Oct}$  or  $P_{md}$ —prior to and during the drought) by controlling daytime declines in leaf water potential (Fig. 1). In the following section, we discuss evidence suggesting that the unexpectedly high leaf water potential (and therefore safety margins) during the drought was linked to stomatal control.

### Coordination between stomatal control and water status in Amazon canopy trees

We found that stomatal control is key for keeping leaf water potential of central Amazon trees at safe levels to avoid dehydration during extreme droughts. Many studies have already shown the importance of stomatal function as an important mechanism of water regulation in seasonal droughts (Bonal et al. 2000; Brodribb and Holbrook 2004; Miranda et al. 2005) but only a few studies have been able to assess this question in tropical forests during severe droughts (Skelton et al. 2015; Fontes et al. 2018), or as part of an individual-level trade-off between physiological regulation and structural embolism resistance. We show for the first time that under a natural extreme drought, individual canopy rainforest trees exhibit strong stomatal regulation that coordinated with embolism resistance acts to prevent dehydration.

Specifically, we first note that the minimum daily water potential during 2015 seasonal evolution ( $P_{\min}$ ) did not always occur at midday ( $P_{md}$ ) or during seasonal drought peak ( $P_{\min|Oct}$ ). Second, the lower predawn leaf water potential during the dry season (Fig. 1, upper left panel) clearly indicates that the drought-induced reduction in the soil water content (Fig. S4b) affected tree water status overall, but tree responses varied depending on the degree of stomatal control coordinated with xylem condition. (i) The less negative than expected minimum daytime xylem water potential at the drought peak ( $P_{\min|Oct}$ ) appears to be associated with trees that had lower stomatal conductance during the drought (Fig. 3a, left side) that prevented water loss and dehydration. As  $P_{\min|Oct}$  was also found to be associated with embolism resistance ( $P_{50}$ ) (Fig. 2e), this suggests an indirect coordination of stomatal regulation with xylem safety characteristics: trees that can maintain higher stomatal conductance (and thus endure more

negative  $P_{\min|Oct}$ ) during an extreme drought are also those that invest in a more resistant hydraulic system (Fig. 2e; Fig. S6a, b). (ii) We found a direct relationship between a wet-to-dry season reduction in stomatal conductance with xylem vulnerability characteristics – the embolism starting point  $P_{12}$  (Fig. 3b). The interpretation is that trees partially closed their stomata (which allowed to reduce xylem tension) likely as a feedback mechanism, to avoid further tissue embolization due to transpiration water loss and the corresponding drop in water potential. Trees with xylem more prone to cavitation (i.e., less negative  $P_{12}$ ) adjusted their stomatal conductance more strongly to keep hydraulic integrity at safe levels (Fig. 3b). These inferences on concerted coordination between stomatal response ( $g_s$ ,  $\delta g_s$ ) and xylem intrinsic characteristics ( $P_{50}$ ,  $P_{12}$ ) and the state of hydration ( $P_{\min}$ ,  $P_{md}$  and  $P_{\min|Oct}$ ) as well as the large hydraulic safety margins suggest a conservative strategy exhibited during a strong natural drought by these top canopy forest species.

As a consequence of stomatal control, plants incurred some cost in terms of carbon gain, but it was partially mitigated by the seasonal increase in water-use efficiency for most trees. The photosynthetic rate declined proportionally less than transpiration, increasing the iWUE (Fig. 2f), as expected, stomatal control to maintain the state of hydration did not necessarily imply proportionally the same impact on the efficiency of carbon gain, even though the total uptake was reduced. Understanding whether such a linkage exists is however especially important for Amazonian trees because there have been reports showing low hydraulic regulation in response to average drought conditions (e.g., by stomata in Domingues et al. 2010; Rowland et al. 2015b). This would imply that trees can predominantly rely on xylem architecture to cope with abnormal drought conditions; here, we suggest this might not be the case and that hydraulic regulation, including directly observed stomatal regulation (Fig. 3), plays a significant role in protecting more embolism-vulnerable plants from drought.

The extreme 2015 *El Niño* event conditions were particularly useful to address the role of stomatal regulation in controlling transpiration rates and, as a result, keeping the xylem tension at safe levels. During the drought, maximum VPD increased by over 100%: from 2.1 kPa during the preceding wet period, to 4.4 kPa during the peak of the drought period. The dry atmosphere, in combination with the low soil water content and increasing embolism levels, triggered a stomatal response that prevented the occurrence of even lower  $P_{\min|Oct}$ . Specifically, plants with high resistance to embolism could maintain high transpiration and  $\text{CO}_2$  uptake, but also showed reduction of these rates. For example, the studied *Swartzia tomentifera* tree exhibits high embolism resistance ( $P_{50} = -3.05$  MPa) but also had a high stomatal reduction and transpiration, reinforcing the idea that

occurrence of embolism in the field was the trigger for the regulatory response, including observed stomatal responses.

Overall, the main mechanisms previously suggested to explain the high forest resistance to drought in tropical climates were: deep rooting, soil niches for water uptake, high embolism resistance for plateau species, the redistribution of water in the soil, and direct water uptake by leaves during dry season rains and nighttime dew events (Nepstad et al. 1994; Oliveira et al. 2005; Hole et al. 2007; Ivanov et al. 2012; Binks et al. 2016; Brum et al. 2019). Here we found evidence for an additional key mechanism: strong coordination between the state of xylem hydration and the degree of hydraulic and stomatal regulation, which result in higher xylem safety. The prevalence of drought resistance traits across different taxa suggest that past drought events likely shaped trait evolution of central Amazonian trees.

### Height-structured trade-offs between embolism resistance and stomatal regulation

We found evidence that in central Amazonian trees this trade-off between embolism resistance and stomatal regulation is height-structured. Specifically, tree embolism resistance ( $P_{50}$ ) decreased with tree height and DBH, but increased with wood density (Fig. 4a–d). Concurrently, the level of stomatal control increased with tree height, suggesting trade-offs between investment in xylem and reliance on active stomatal regulation. That is, given the 2015 drought impact on soil water potential, taller trees were more vulnerable to embolism (less negative  $P_{50}$ ) but exhibited a higher degree of stomatal conductance reduction (Fig. 4c). Evidence for a height-structured relationship has already been presented at this site (Santos et al. 2018), showing smaller stomatal conductance reductions in under-story trees. Even for xylem tissues with lower risk of experiencing a high level of embolism, we show that the response was associated not only with xylem traits (such as  $P_{50}$ ), but also with the ability of trees to regulate stomatal closure during drought to prevent tissue dehydration. This finding of a height-structured trade-off is consistent with other height-structured trade-offs such as root niche segregation, proposed for a site in eastern Amazonia (Ivanov et al. 2012; Brum et al. 2019).

Previous research has demonstrated that taller trees are more susceptible to mortality during droughts (Bennett et al. 2015). This suggests that the long hydraulic path and exposure to a drier atmosphere likely result in a drastic reduction of whole-tree conductance, placing the oldest and biggest Amazonian trees in imminent risk of drought-induced mortality (McDowell and Allen 2015). Nonetheless, another study provided evidence that mortality during extreme droughts in the Colombian Amazon is not structured by height but by wood density and hydrological environment (Zuleta et al. 2017). Our results support both previous observations: we found a relationship between the embolism resistance with

both tree height and wood density (Fig. 4a, d). The evidence of wood-property and tree-height structured relationships coupled with the tight coordination between stomatal regulation and hydraulic vulnerability highlight the complexity of tropical tree responses to droughts and calls for further research on whole-plant regulation mechanisms.

### Conclusion

Overall, contrary to our initial expectation, trees in central Amazon operated far from their hydraulic limits when exposed to an extreme natural drought, thereby exhibiting a hydraulic conservative strategy. Specifically, increases in stem embolism might have acted as a feedback mechanism triggering the stomatal closure to avoid further embolism, while explaining declines in photosynthesis and transpiration. Here, we present clear evidence of coordination between stomatal and hydraulic traits at the level of individual trees, a finding that has been expected but not yet clearly demonstrated or quantified for tropical trees during natural droughts. This coordination is likely to have important implications for the regulation of carbon and water balance at large scales. We expect that the hydraulic mechanisms implied by such coordination should be useful for developing more accurate model predictions of ecosystem-scale responses to droughts across the Amazon region.

**Supplementary Information** The online version contains supplementary material available at <https://doi.org/10.1007/s00442-021-04924-9>.

**Acknowledgements** We thank the National Institute of Amazon Research (INPA) and the Large-Scale Biosphere-Atmosphere experiment (LBA) for logistical support. MJF and RSO thanks CNPq for a productivity scholarship.

**Author contribution statement** MNG, RSO, and MJF designed the research. MNG, VAHFS, AVG, and JVBC collected the data. MNG analyzed the data. MNG, SVCM, SRS, and VI interpreted the analyses. MNG wrote the first draft and RSO, MJF, SVCM, SRS, VAHFS, and VI authors contributed to editing the manuscript.

**Funding** This work was supported by the GOAmazon project, jointly funded by the Brazilian Research Foundations of São Paulo State (FAPESP #13/50533-5), and Amazonas State (FAPEAM #062.00570/2014), and the U.S. Department of Energy (awards SC0008383 and SC0011078). Also, we acknowledge additional support by the U.S. National Science Foundation (award #1754803) and Brazil's Coordination of Improvement of Higher Level Personnel (CAPES).

### References

Aleixo I, Norris D, Hemerik L et al (2019) Amazonian rainforest tree mortality driven by climate and functional traits. *Nat Clim Change* 9:384–388. <https://doi.org/10.1038/s41558-019-0458-0>

Allen CD, Breshears DD, McDowell NG (2015) On underestimation of global vulnerability to tree mortality and forest die-off from hotter drought in the Anthropocene. *Ecosphere* 6:1–55. <https://doi.org/10.1890/ES15-00203.1>

Anderegg WRL, Klein T, Bartlett M et al (2016) Meta-analysis reveals that hydraulic traits explain cross-species patterns of drought-induced tree mortality across the globe. *Proc Natl Acad Sci U S A* 113:5024–5029. <https://doi.org/10.1073/pnas.1525678113>

Anderegg WRL, Wolf A, Arango-Velez A et al (2018) Woody plants optimise stomatal behaviour relative to hydraulic risk. *Ecol Lett* 21:968–977

Aragão LEOC, Malhi Y, Roman-Cuesta RM et al (2007) Spatial patterns and fire response of recent Amazonian droughts. *Geophys Res Lett* 34:1–5. <https://doi.org/10.1029/2006GL028946>

Araújo AC, Nobre AD, Kruijt B et al (2002) Comparative measurements of carbon dioxide fluxes from two nearby towers in a central Amazonian rainforest: the Manaus LBA site. *J Geophys Res* 107:8090. <https://doi.org/10.1029/2001JD000676>

Bates D, Maechler M (2007) Linear mixed-effects models using *S4* classes. *R Package Version 2:74*

Bennett AC, McDowell NG, Allen CD et al (2015) Drought-induced mortality patterns and rapid biomass recovery in a terra firme forest in the Colombian Amazon. *Nat Plants* 1:1–5. <https://doi.org/10.1002/ecy.1950>

Binks O, Meir P, Rowland L et al (2016) Plasticity in leaf-level water relations of tropical rainforest trees in response to experimental drought. *New Phytol* 211:477–488. <https://doi.org/10.1111/nph.13927>

Bonal D, Barigah TS, Granier A, Guehl JM (2000) Late-stage canopy tree species with extremely low  $\delta^{13}\text{C}$  and high stomatal sensitivity to seasonal soil drought in the tropical rainforest of French Guiana. *Plant Cell Environ* 23:445–459. <https://doi.org/10.1046/j.1365-3040.2000.00556.x>

Brienen RJW, Phillips OL, Feldpausch TR et al (2015) Long-term decline of the Amazon carbon sink. *Nature* 519:344–348. <https://doi.org/10.1038/nature14283>

Brodrribb TJ, Holbrook NM (2004) Diurnal depression of leaf hydraulic conductance in a tropical tree species. *Plant Cell Environ* 27:820–827. <https://doi.org/10.1111/j.1365-3040.2004.01188.x>

Brum M, Vadeboncoeur MA, Ivanov V et al (2019) Hydrological niche segregation defines forest structure and drought tolerance strategies in a seasonal Amazon forest. *J Ecol* 107:318–333. <https://doi.org/10.1111/1365-2745.13022>

Chmura DJ, Guzicka M, McCulloh KA, Zytkowiak R (2015) Limited variation found among Norway spruce half-sib families in physiological response to drought and resistance to embolism. *Tree Physiol* 36:252–266. <https://doi.org/10.1093/treephys/tpv141>

Choat B, Jansen S, Brodrribb TJ et al (2012) Global convergence in the vulnerability of forests to drought. *Nature* 491:752–755. <https://doi.org/10.1038/nature11688>

Crowther TW, Glick HB, Covey KR et al (2015) Mapping tree density at a global scale. *Nature* 525:201–205. <https://doi.org/10.1038/nature14967>

Cuarteras LA, Tomasella J, Nobre AD et al (2012) Distributed hydrological modeling of a micro-scale rainforest watershed in Amazonia: model evaluation and advances in calibration using the new HAND terrain model. *J Hydrol* 462–463:15–27. <https://doi.org/10.1016/j.jhydrol.2011.12.047>

de Barros FV, Bittencourt PRL, Brum M et al (2019) Hydraulic traits explain differential responses of Amazonian forests to the 2015 El Niño-induced drought. *New Phytol* 223:1253–1266. <https://doi.org/10.1111/nph.15909>

Domingues TF, Meir P, Feldpausch TR et al (2010) Co-limitation of photosynthetic capacity by nitrogen and phosphorus in West Africa woodlands. *Plant Cell Environ* 33:959–980. <https://doi.org/10.1111/j.1365-3040.2010.02119.x>

dos Santos VAHF, Ferreira MJ, Rodrigues JVFC et al (2018) Causes of reduced leaf-level photosynthesis during strong El Niño drought in a Central Amazon forest. *Glob Change Biol* 24:4266–4279. <https://doi.org/10.1111/gcb.14293>

Doughty CE, Metcalfe DB, Girardin CAJ et al (2015) Drought impact on forest carbon dynamics and fluxes in Amazonia. *Nature* 519:78–82. <https://doi.org/10.1038/nature14213>

Fauset S, Johnson MO, Gloor M et al (2015) Hyperdominance in Amazonian forest carbon cycling. *Nat Commun* 6:1–9. <https://doi.org/10.1038/ncomms7857>

Fauset S, Gloor M, Fyllas NM et al (2019) Individual-based modeling of Amazon forests suggests that climate controls productivity while traits control demography. *Front Earth Sci* 7:1–19. <https://doi.org/10.3389/feart.2019.00083>

Fettig CJ, Mortenson LA, Bulaon BM, Foulk PB (2019) Tree mortality following drought in the central and southern Sierra Nevada, California, U.S. *For Ecol Manage* 432:164–178. <https://doi.org/10.1016/j.foreco.2018.09.006>

Field A (2018) Discovering Statistics Using IBM SPSS Statistics

Fontes CG, Dawson TE, Jardine K et al (2018) Dry and hot: the hydraulic consequences of a climate change-type drought for Amazonian trees. *Philos Trans R Soc B Biol Sci*. <https://doi.org/10.1098/rstb.2018.0209>

Hernandez-Santana V, Rodriguez-Dominguez CM, Fernández JE, Diaz-Espejo A (2016) Role of leaf hydraulic conductance in the regulation of stomatal conductance in almond and olive in response to water stress. *Tree Physiol* 36:725–735. <https://doi.org/10.1093/treephys/tpv146>

Hole W, Nepstad DC, Tohver IM et al (2007) Mortality of large trees and lianas following experimental drought in an Amazon forest. *Ecol Soc Am* 88:2259–2269

Ivanov VY, Hutyra LR, Wofsy SC et al (2012) Root niche separation can explain avoidance of seasonal drought stress and vulnerability of overstory trees to extended drought in a mature Amazonian forest. *Water Resour Res* 48:1–21. <https://doi.org/10.1029/2012WR011972>

Jiménez-Muñoz JC, Mattar C, Barichivich J et al (2016) Record-breaking warming and extreme drought in the Amazon rainforest during the course of El Niño 2015–2016. *Sci Rep* 6:1–7. <https://doi.org/10.1038/srep33130>

Li L, McCormack ML, Ma C et al (2015) Leaf economics and hydraulic traits are decoupled in five species-rich tropical-subtropical forests. *Ecol Lett* 18:899–906. <https://doi.org/10.1111/ele.12466>

Lloyd J, Farquhar GD (2008) Effects of rising temperatures and  $[\text{CO}_2]$  on the physiology of tropical forest trees effects of rising temperatures and  $[\text{CO}_2]$  on the physiology of tropical forest trees. *Philos Trans R Soc* 363:1811–1817. <https://doi.org/10.1098/rstb.2007.0032>

Malhi Y, Nobre AD, Grace J et al (1998) Carbon dioxide transfer over a Central Amazonian rain forest. *J Geophys Res Atmos* 103:31593–31612. <https://doi.org/10.1029/98JD02647>

Malhi Y, Aragão LEOC, Galbraith D et al (2009) Exploring the likelihood and mechanism of a climate-change-induced dieback of the Amazon rainforest. *PNAS* 106:20611–20615. <https://doi.org/10.1073/pnas.0804619106>

McDowell NG, Allen CD (2015) Darcy's law predicts widespread forest mortality under climate warming. *Nat Clim Change* 5:669–672. <https://doi.org/10.1038/nclimate2641>

McDowell NG, Williams AP, Xu C et al (2015) Multi-scale predictions of massive conifer mortality due to chronic temperature rise. *Nat Clim Change* 6:295–300. <https://doi.org/10.1038/nclimate2873>

McDowell N, Allen CD, Anderson-Teixeira K et al (2018) Drivers and mechanisms of tree mortality in moist tropical forests. *New Phytol* 219:851–869. <https://doi.org/10.1111/nph.15027>

Miranda EJ, Vourlitis GL, Filho NP et al (2005) Seasonal variation in the leaf gas exchange of tropical forest trees in the rain

forest—savanna transition of the southern Amazon Basin How to cite this article: seasonal variation in the leaf gas exchange of tropical forest trees. *J Trop Ecol* 21:451–460. <https://doi.org/10.1017/S0266467405002427>

Mitchell PJ, Grady APO, Tissue DT et al (2013) Drought response strategies define the relative contributions of hydraulic dysfunction and carbohydrate depletion during tree mortality. *New Phytol* 197:862–872. <https://doi.org/10.1111/nph.12064>

Nepstad DC, de Carvalho CR, Davidson EA et al (1994) The role of deep roots in the hydrological and carbon cycles of Amazonian forests and pastures. *Nature* 372:666–669

Oliveira RS, Dawson TE, Burgess SSO, Nepstad DC (2005) Hydraulic redistribution in three Amazonian trees. *Oecologia* 145:354–363. <https://doi.org/10.1007/s00442-005-0108-2>

Pereira L, Bittencourt PRL, Oliveira RS et al (2016) Plant pneumatics: stem air flow is related to embolism - new perspectives on methods in plant hydraulics. *New Phytol* 211:357–370. <https://doi.org/10.1111/nph.13905>

Phillips OL, Aragao LEOC, Lewis SL et al (2009) Drought sensitivity of the Amazon rainforest. *Science* 323:1344–1347. <https://doi.org/10.1126/science.1164033>

Phillips OL, van der Heijden G, Lewis SL et al (2010) Drought-mortality relationships for tropical forests. *New Phytol* 187:631–646. <https://doi.org/10.1111/j.1469-8137.2010.03359.x>

Powers JS, Vargas GG, Brodribb TJ et al (2020) A catastrophic tropical drought kills hydraulically vulnerable tree species. *Glob Chang Biol* 26:3122–3133. <https://doi.org/10.1111/gcb.15037>

Pratt RB, Castro V, Fickle JC, Jacobsen AL (2020) Embolism resistance of different aged stems of a California Oak species (*Quercus Douglasii*): optical and microCT methods differ from the bench-top-dehydration standard. *Tree Physiol* 40(1):5–18

R Development Core Team (2011) R: a language and environment for statistical computing. R Foundation for Statistical Computing, Vienna, Austria. <http://www.R-project.org/> (ISBN 3-900051-07-0)

Resco V, Ewers BE, Sun W et al (2009) Drought-induced hydraulic limitations constrain leaf gas exchange recovery after precipitation pulses in the C3 woody legume, *Prosopis velutina*. *New Phytol* 181:672–682. <https://doi.org/10.1111/j.1469-8137.2008.02687.x>

Rowland L, Da Costa APLL, Galbraith DR et al (2015a) Death from drought in tropical forests is triggered by hydraulics not carbon starvation. *Nature* 528:1–13. <https://doi.org/10.1038/nature15539>

Rowland L, Lobo-do-Vale RL, Christoffersen BO et al (2015b) After more than a decade of soil moisture deficit, tropical rainforest trees maintain photosynthetic capacity, despite increased leaf respiration. *Glob Chang Biol* 21:4662–4672. <https://doi.org/10.1111/gcb.13035>

Saleska SR, Didan K, Huete AR, Rocha HR (2007) Amazon forests green-up during 2005 drought. *Science* 318:2007–2007. <https://doi.org/10.1126/science.1146663>

Scholander PF, Hammel HT, Bradstreet D, Hemmingsen EA (1964) Sap pressure in vascular plants negative hydrostatic pressure can be measured in plants. *Science* 148:339–346

Skelton RP, West AG, Dawson TE (2015) Predicting plant vulnerability to drought in biodiverse regions using functional traits. *Proc Natl Acad Sci U S A* 112:5744–5749. <https://doi.org/10.1073/pnas.1503376112>

Sombroek W (2001) Spatial and temporal patterns of Amazon rainfall. *BioOne* 30:388–396. <https://doi.org/10.1579/0044-7447-30.7.388>

Sperry JS (2000) Hydraulic constraints on plant gas exchange. *Agric For Meteorol* 104:13–23. [https://doi.org/10.1016/S0168-1923\(00\)00144-1](https://doi.org/10.1016/S0168-1923(00)00144-1)

Sperry JS, Love DM (2015) What plant hydraulics can tell us about responses to climate-change droughts. *New Phytol* 207:14–27. <https://doi.org/10.1111/nph.13354>

Stpaul NKM, Limousin JM, Rodríguez-Calcerrada J et al (2012) Photosynthetic sensitivity to drought varies among populations of *Quercus ilex* along a rainfall gradient. *Funct Plant Biol* 39:25–37. <https://doi.org/10.1071/FP11090>

ter Steege H, Pitman NCA, Sabatier D et al (2013) Hyperdominance in the Amazonian Tree Flora. *Science* 342:1243092–1243092. <https://doi.org/10.1126/science.1243092>

Turner NC (1981) Techniques and experimental approaches for the measurement of plant water status. *Plant Soil* 58(1):339–366. <https://doi.org/10.1007/BF02180062>

Venturas MD, MacKinnon ED, Dario HL, Jacobsen AL, Brandon Pratt R, Davis SD (2016) Chaparral shrub hydraulic traits, size, and life history types relate to species mortality during California's Historic Drought of 2014. *PLoS ONE* 11(7):e0159145

Wang Y, Sperry JS, Anderegg WRL et al (2020) A theoretical and empirical assessment of stomatal optimization modeling. *New Phytol* 227:311–325. <https://doi.org/10.1111/nph.16572>

Wu J, Serbin SP, Ely KS et al (2019) The response of stomatal conductance to seasonal drought in tropical forests. *Glob Chang Biol* 81:gcb14820. <https://doi.org/10.1111/gcb.14820>

Zhang Y, Lamarque LJ, Torres-Ruiz JM et al (2018) Testing the plant pneumatic method to estimate xylem embolism resistance in stems of temperate trees. *Tree Physiol* 38:1016–1025. <https://doi.org/10.1093/treephys/tpy015>

Ziegler C, Coste S, Stahl C et al (2019) Large hydraulic safety margins protect Neotropical canopy rainforest tree species against hydraulic failure during drought. *Ann For Sci.* <https://doi.org/10.1007/s13595-019-0905-0>

Zuleta D, Duque A, Cardenas D et al (2017) Drought-induced mortality patterns and rapid biomass recovery in a terra firme forest in the Colombian Amazon. *Ecology* 98:2538–2546. <https://doi.org/10.1002/ecy.1950>